Vol 18 No 4, April 2009
1674-1056/2009/18(04)/1637-06

Chinese Physics B

© 2009 Chin. Phys. Soc.
and IOP Publishing Ltd

Raman scattering studies on manganese ion-implanted GaN*

Xu Da-Qing(徐大庆)†, Zhang Yi-Men(张义门), Zhang Yu-Ming(张玉明), Li Pei-Xian(李培咸), and Wang Chao(王 超)

Key Laboratory of Ministry of Education for Wide Band-Gap Semiconductor Materials and Devices, School of Microelectronics, Xidian University, Xi'an 710071, China

(Received 7 October 2008; revised manuscript received 5 November 2008)

This paper reports that the Raman spectra have been recorded on the metal-organic chemical vapour deposition epitaxially grown GaN before and after the Mn ions implanted. Several Raman defect modes have emerged from the implanted samples. The structures around 182 cm^{-1} modes are attributed to the disorder-activated Raman scattering, whereas the 361 cm^{-1} and 660 cm^{-1} peaks are assigned to nitrogen vacancy-related defect scattering. One additional peak at 280 cm^{-1} is attributed to the vibrational mode of gallium vacancy-related defects and/or to disorder activated Raman scattering. A Raman-scattering study of lattice recovery is also presented by rapid thermal annealing at different temperatures between 700 °C and 1050 °C on Mn implanted GaN epilayers. The behaviour of peak-shape change and full width at half maximum (FWHM) of the A_1(LO) (733 cm^{-1}) and E_2^H (566 cm^{-1}) Raman modes are explained on the basis of implantation-induced lattice damage in GaN epilayers.

Keywords: diluted magnetic semiconductors, gallium nitride, implantation, Raman spectroscopy
PACC: 7550P, 7280E, 6170T, 7830

1. Introduction

Diluted magnetic semiconductors (DMSs) have attracted great interest in exploiting the spin of charge carriers in semiconductors because of their potential application to new devices based on spin polarized transport or integration of magnetic, optical, and electronic functions on a single chip. Mn-doped GaN materials are good materials for obtaining a Curie temperature (T_c) higher than room temperature according to the theoretical calculation.[1] Mn ions are usually introduced into GaN either during growth or by ion implantation. A major obstacle to form DMSs material GaN:Mn has been the low solubility of manganese elements in GaN. Advantages of ion implantation are the selective doping of certain areas on the sample, the precise control of dopant concentration and depth distribution, and the introduction of a large number of elements without any limitation of solubility. Despite the fact that GaN is a host of very robust semiconductor, damage of the crystal lattice is induced by the implantation which must be removed by subsequent thermal annealing. Although some experimental studies on the GaN-based DMS have been reported, most of the reports deal only with magnetic characteristics of Mn ion-implanted GaN[2−5] rather than with structural properties. To our knowledge, few reports are available about the Raman scattering studies on structural properties of Mn-implanted GaN with different post-annealing temperatures.

Raman scattering is a powerful, non-destructive technique to assess more useful information about the crystalline quality and other important properties of semiconductor crystals. Raman scattering technique is also very sensitive to ion implantation-induced defects and any irregularity in the crystalline symmetry. As GaN is transparent to the incident laser beam, it is possible to analyse the entire region of GaN implanted by Mn ions. In this paper, we have studied the effect of Mn implantation in the GaN lattice vibrations and analysed the characterization of lattice recovery in Mn ions implanted GaN epilayers for different annealing conditions using Raman scattering.

2. Experimental

The implantations were carried out on 3 μm thick unintentionally doped GaN epilayers which were

*Project supported by the National Natural Science Foundation of China (Grant No 90407014).
†E-mail: dqxu@mail.xidian.edu.cn

grown by metal-organic chemical vapour deposition (MOCVD) at about 950 °C, after a 25 nm GaN buffer grown firstly at a substrate temperature of 540 °C. For comparison, two groups of GaN samples were studied after implantation. One set of samples named "A" was implanted at room temperature with Mn ions, using an ion-beam energy of 300 keV with doses of $4.67\times10^{16}\,\mathrm{cm}^{-2}$ resulting in a maximum concentration of about $4\times10^{21}\,\mathrm{cm}^3$. The other set of samples named "B" was implanted with multiple energy Mn ions implantation to produce well-proportioned concentrations about $3\times10^{21}\,\mathrm{cm}^3$ in the top 300 nm of the GaN. Implantation energies, ion average range and ion fluences of Mn ions in these two sets of samples are given in Table 1 and Table 2 calculated with TRIM98. To achieve impurity activation and lattice recovery, these two sets were annealed at 700 °C, 800 °C, 900 °C for 5 min and at 1050 °C for 2 min in the ambience flowing N_2 gas with the samples faced down on GaN wafers respectively.

Table 1. Manganese ion implantation used for sample A.

ion energy/keV	ion average range/nm	ion fluence/cm^{-2}
300	127.09	4.6717×10^{16}

Table 2. Manganese ion implantation used for sample B.

ion energy/keV	ion average range/nm	ion fluence/cm^{-2}
60	27.484	9.16025×10^{15}
200	84.668	2.4870×10^{16}
500	214.57	5.3618×10^{16}

The Raman measurements were carried out at room temperature using the 514.5 nm line of an Ar laser as an excitation source. The laser beam was focused by a microscope lens system with a 50× objective lens yielding a spot diameter of 2 μm. The scattered light was detected in backscattering geometry using a Renishaw-RM2000 model spectrometer with a CCD detector.

3. Results and discussion

For wurtzite GaN and for the wave vector $k = 0$, group theory predicts eight vibrational modes $2A_1+2B_1+2E_1+2E_2$, of which one A_1, one E_1 and two E_2 are Raman active. One set of A_1 and one set of E_1 correspond to acoustic phonons and the B_1 modes are silent. Due to LO±TO splitting, GaN has six Raman-active optical modes namely A_1(TO), E_1(TO), A_1(LO), E_1(LO) and $2E_2$ in various scattering geometries.[6] Figure 1 shows the Raman spectrum of as-grown GaN epilayers. For the as-grown sample, the A_1(LO)(733 cm^{-1}) and E_2^{H} (566 cm^{-1}) are observed as expected from the Raman selection rules in wurtzite GaN films[7]. The peaks at 416 cm^{-1} and 747 cm^{-1} stem from the sapphire substrate.

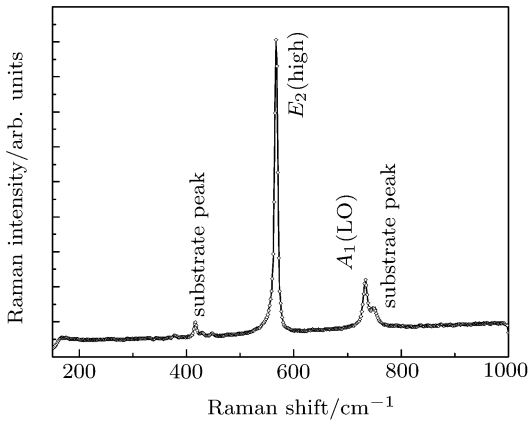


Fig.1. The room temperature Raman spectra of as-grown GaN epitaxial layer on sapphire substrate in the backscattering geometry. The labels of the peaks denote the Raman active modes.

The implantation-induced defects can affect the Raman spectra in the following two distinct ways: (1) defects can induce additional Raman structures due to local vibrational modes or via electronic transitions (electronic Raman scattering); (2) defects can activate the intrinsic Raman modes, which are normally forbidden or silent due to the breakdown of selection rules in disordered materials. At high-defect density, wave vector conservation in the Raman scattering process breaks down, and phonons from the entire Brillouin zone can be observed in the Raman spectrum. Thus, the Raman spectrum exhibits the total phonon density of states. This phenomenon is called disorder-activated Raman scattering (DARS).[8] While the exact nature of the implantation-induced peaks in the Raman spectra of implanted GaN is still a debated subject, they are mainly categorized into: i) DARS; ii) scattering mechanisms of implantation induced defects, such as interstitials, vacancies, or antisites, in the host lattice.

Figure 2 shows the Raman spectra of Mn-implanted epilayers and subsequent annealing at temperatures of 700 °C, 800 °C, 900 °C for 5 min and 1050 °C for 2 min. For contrast, Raman spectrum of the as grown sample is also shown at the bottom of Fig.2. The Raman spectra show a notable intensity decrease of the A_1(LO) and $E_2^{\rm H}$ modes after Mn-implanted, but no obvious frequency change was detected. Additional modes can be observed at 182, 280, 361 and 660 $\rm cm^{-1}$. The intensities of the A_1(LO) and E_2^H increase with annealing temperature. The intensities of the $\rm P_1$ mode at 182 $\rm cm^{-1}$ and the $\rm P_2$ mode at 280 $\rm cm^{-1}$ decrease with increasing annealing temperature from 700∼900 °C, and the $\rm P_2$ mode nearly disappears at 900 °C. On the contrary, the $\rm P_3$ mode at 361 $\rm cm^{-1}$ and the $\rm P_4$ mode at 660 $\rm cm^{-1}$ exhibit a pronounced intensity increase at 900 °C. With increasing annealing temperature their intensities also drop but the modes are still visible at 1050 °C. It is believed that the $\rm Ga_xMn_y$ phases are formed after Mn-implanted undoped GaN epilayers being annealed at 700 and 800 °C.[9] The $\rm Ga_xMn_y$ phases could lead to the formation of Ga vacancies. The Ga-Mn phases reduced drastically as annealing temperature increased to 900 °C. This is due to the fact that Mn preferentially interacted with N atoms to precipitate the Mn-N phases. Increasing the annealing temperature to 900 °C promoted the formation of $\rm Mn_xN_y$ compounds, this compounds in GaN should change the surroundings into nitrogen-deficient condition, leading to the formation of N vacancies. It is also well known that the energetic Mn ions penetrating through a GaN film generate a collision cascade, which consists of vacancies in the gallium and nitrogen sublattices ($\rm V_{Ga}$ and $\rm V_N$), gallium and nitrogen interstitials ($\rm Ga_{\it i}$ and $\rm N_{\it i}$), and the antisite defects. Some of these implantation-produced defects can be removed by annealing below 900 °C. But the N vacancy-related defects increase very rapidly by annealing above 900 °C because the decomposition of GaN at high temperature causes the loss of nitrogen from the GaN surface. On the other hand, the density of state (DOS) spectrum in the energy region of $\rm P_3$ peak and $\rm P_4$ peak is dominated by nitrogen atoms motions,[10,11] and in the energy region of $\rm P_2$ peak, the phonon DOS is dominated by the motions of Ga atoms.[10,11] Therefore, from the observed annealing behaviour of the Raman intensities and for the reason above, we find that the $\rm P_3$ peak at 361 $\rm cm^{-1}$ and the $\rm P_4$ peak at 660 $\rm cm^{-1}$ originate from the vibrational mode of nitrogen vacancy-related defects, and the $\rm P_2$ peak at 280 $\rm cm^{-1}$, besides some contributions from DARS, the contribution related to scattering processes from Ga vacancy-related defects cannot be excluded. The broad structure centre around 182 $\rm cm^{-1}$ may result from a DARS, where built-in defects yield a relaxation of the $k = 0$ selection rule for Raman scattering, and phonons from the whole Brillouin zone can be observed. Some similar observations have been made by many authors in the Raman spectra of GaN samples implanted with Mg, Ar, P, C, Ca, Si, Er, O and N ions.[12−15]

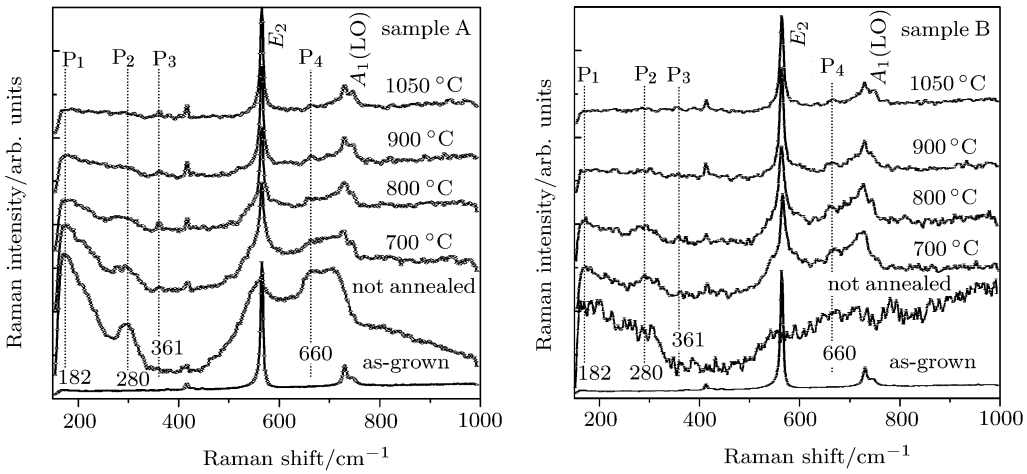


Fig.2. The room temperature Raman spectra of as-grown and Mn ions implanted GaN epitaxial layer annealed at different temperatures.

Figure 3 shows the peaks of A_1 (LO) and E_2^H modes for Mn-implanted GaN samples annealed at different temperatures. As can be seen from the spectra, a relatively high degree of lattice recovery is achieved in the annealing temperature T_A of 700 °C. However, the intense peaks of A_1 (LO) and E_2^H modes detected exhibit a clear asymmetry with a low-energy tail and a large full width at half maximum (FWHM), as shown in Fig.4, which is indicative of the participation of $k \neq 0$ modes (DARS) and hence of a significant residual implantation damage in the GaN lattice. This is also confirmed by the presence of a broad intense band around the P_1 mode at 182 cm^{-1} in Fig.2, which is associated with DARS. As can be seen in Fig.3 the A_1 (LO) and E_2^H peaks become more intense and exhibit a decrease in their FWHMs for increasing T_A up to 900 °C, as shown in Fig.4. These changes in the A_1 (LO) and E_2^H peaks show the gradual recovery of long-range ordering in the GaN lattice that implies a more stringent verification of the $k = 0$ selection rule for Raman scattering, drastically reducing the participation of phonons with $k \neq 0$. The peak at the P_1 mode at 182 cm^{-1} shows a parallel intensity decrease with T_A, as shown in Fig.2. The weak intensity of the P_1 signal is a clear evidence of the excellent crystallinity recovery which is achieved by rapid thermal annealing (RTA).

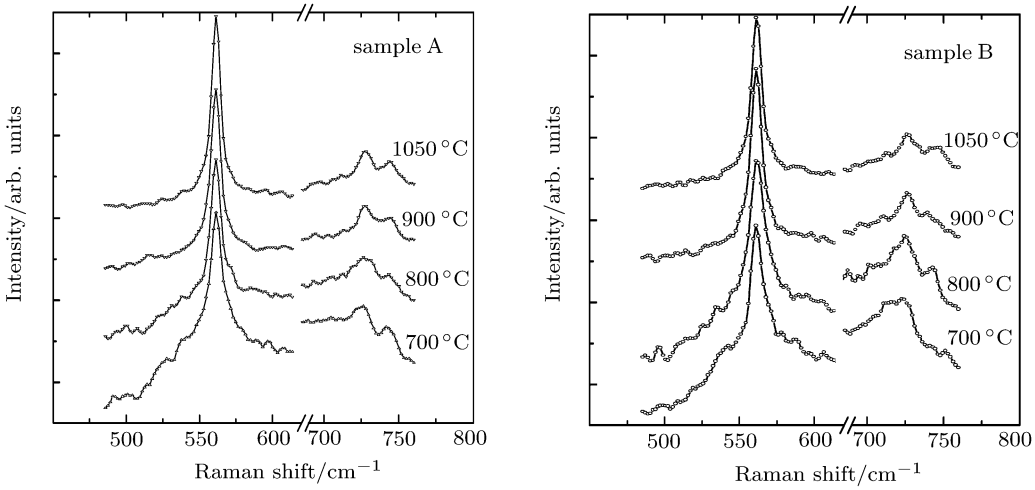


Fig.3. The peaks of A_1 (LO) and E_2^H modes for Mn-implanted GaN samples annealed at different temperatures.

In Fig.4 we evaluate the degree of lattice recovery in the annealed samples by plotting FWHM of E_2^H and A_1 (LO) modes As can be seen in Fig.4 the FWHMs of E_2^H and A_1 (LO) modes rapidly decrease from ≈11.5 cm^{-1} and 13.6 cm^{-1} at T_A=700 °C to 7.6 cm^{-1} and 8.7 cm^{-1} at T_A=1050 °C for sample A, and similarly, from ≈12.1 cm^{-1} and 20.5 cm^{-1} at T_A=700 °C to 8.5 cm^{-1} and 9.7 cm^{-1} at T_A=1050 °C for sample B. The decrease of FWHM is accompanied by a remarkable reduction of the peak asymmetry as shown in Fig.3. These results suggest a fast recovery of the phonon coherence length for relatively low annealing temperatures, though some degree of mis-orientation and/or polycrystalline regions still persists at T_A=700 °C (see the intensity of the 182 cm^{-1} mode in Fig.2). Nevertheless, the P_1 signal at 182 cm^{-1} is visibly reduced in the sample annealed at 900 °C (in Fig.2), indicating an excellent lattice recovery. Only a minor decrease of the E_2^H and A_1 (LO) mode width and asymmetry is achieved by further increasing T_A from 900 °C up to 1050 °C. This may be due to the surface of GaN beginning to decompose while annealing temperature above 900 °C. The samples of the single and multiple energy Mn implantation show the same tendency.

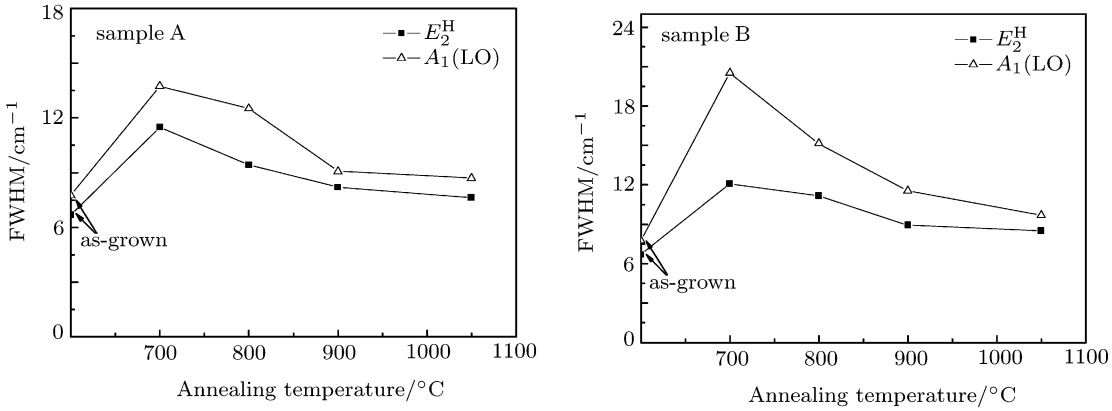


Fig.4. FWHM of E_2^H and A_1(LO) Raman modes of Mn implanted GaN epilayers as a function of annealing temperature.

For Mn-implanted GaN epilayers, another important property concerned here is the ferromagnetic property. In the previous study, we have found that the highest magnetization was obtained from the measurement of the sample annealed at ∼800 °C.[9] Consequently, it is suggested that optimum annealing temperature at 800–900 °C could be an important parameter for reducing the implantation which induced disorders in Mn-implanted GaN films and improving magnetic properties of the films.

4. Conclusions

The Raman measurements were performed on a MOCVD epitaxially grown GaN before and after the implantation with Mn. It is found that Mn ions implantation introduces new Raman peaks in the Raman spectra at frequencies 182, 280, 361, and 660 cm^{-1}. The intensities of the 182 cm^{-1} and the 280 cm^{-1} modes decrease with increasing annealing temperature and the 280 cm^{-1} mode nearly disappears at 900 °C. The intensities of the 361 cm^{-1} mode and the 660 cm^{-1} mode exhibit a pronounced increase at 900 °C and then decreases with increasing annealing temperature in the temperature range from 900 to 1050 °C, but these modes are still visible at 1050 °C. It is proposed that the broad structures of around 182 cm^{-1} modes originate from the DARS. The Raman peaks at 361 cm^{-1} and the 660 cm^{-1} are assigned to the nitrogen vacancy-related defects. The Raman peak at 280 cm^{-1} is attributed to the vibrational mode of gallium vacancy-related defects and/or to DARS.

With increasing annealing temperature we have also observed the gradual recovery of the crystalline features of the Raman spectra of Mn-implanted GaN sample. The evolution of the Raman spectra with T_A suggests the existence of three stages in the lattice recovery process. Firstly, for T_A below 800 °C, the implanted sample starts its recrystallization and restores the crystalline quality. Then, for T_A from 800 °C to 900 °C, there is an increase recovery of the crystalline quality and the decrease of some lattice imperfections in Mn-implanted samples pronounced after annealing. Finally, for T_A above 900 °C, the surface of GaN epilayers begins to decompose. Our results suggest that the optimal lattices recovery and better ferromagnetic properties are achieved by RTA at 800 °C–900 °C.

Acknowledgments

The authors thank Chen Feng-En of Tsinghua University for carrying out the Raman spectra measurements, and also thank Xu Jia-Dong of Institute of Semiconductors, Chinese Academy of Sciences for Mn ion implantation.

References

[1] Dietl T, Ohno H, Matsukura F, Cibert J and Ferrand D 2000 *Science* **287** 1019

[2] Chitta V A, Coaquira J A H, Fernandez J R L, Duarte C A, Leite J R, Schikora D, As D J, Lischka K and Abramof E 2004 *Appl. Phys. Lett.* **85** 3777

[3] Shon Y, Kwon Y H, Yuldashev S U, Park Y S, Fu D J,

Kim D Y, Kim H S and Kang T W 2003 *J. Appl. Phys.* **93** 1546

[4] Baik J M, Shon Y, Kang T W and Lee J L 2004 *Appl. Phys. Lett.* **84** 1120

[5] Theodoropoulou N, Hebard A F, Overberg M E, Abernathy C R, Peartona S J, Chu S N G and Wilson R G 2001 *Appl. Phys. Lett.* **78** 3475

[6] Marcos B, Ibanez J, Cusco R, Martinez F L, Gonzalez-Diaz G and Artus L 2001 *Nuclear Instruments and Methods in Physics Research* B **175** 252

[7] Harima H 2002 *J. Phys.: Condens. Matter* **14** R967

[8] Berg R S, Yu P Y and Weber E R 1985 *Appl. Phys. Lett.* **47** 515

[9] Xu D Q, Zhang Y M, Zhang Y M, Li P X and Wang C (to be published)

[10] Katsikini M, Arvanitidis J, Paloura E C, Ves S, Wendler E and Wesch W 2007 *Opt. Mater.* **29** 1856

[11] Yu Y Y, Zhang R, Xiu X Q, Xie Z L, Yu H Q, Shi Y, Shen B, Gu S L and Zheng Y D 2004 *J. Cryst. Growth* **269** 270

[12] Katsikini M, Papageli K, Paloura E C and Ves S 2003 *J. Appl. Phys.* **94** 4389

[13] Limmer W, Ritter W, Sauer R, Mensching B, Liu C and Rauschenbach B 1998 *Appl. Phys. Lett.* **72** 2589

[14] Song S F, Chen W D, Xu Z J and Xu X R 2007 *Acta Phys. Sin.* **56** 1621 (in Chinese)

[15] Kaschner A, Siegle H, Kaczmarczyk G, Straburg M, Hoffmann A and Thomsen C 1999 *Appl. Phys. Lett.* **74** 3281